Polyhedron xxx (2015) xxx–xxx

Contents lists available at ScienceDirect

Polyhedron

journal homepage: www.elsevier.com/locate/poly

Uranyl(VI) binding by bis(2-hydroxyaryl)diimine and bis(2-hydroxyaryl)diamine ligand derivatives. Synthetic, X-ray, DFT and solvent extraction studies

Harold B. Tanh Jeazet [a], Kerstin Gloe [a], Thomas Doert [a], Jens Mizera [a], Olga N. Kataeva [b], Satoru Tsushima [c], Gert Bernhard [c], Jan J. Weigand [a,*], Leonard F. Lindoy [d,*], Karsten Gloe [a,*]

[a] Department of Chemistry and Food Chemistry, Technical University Dresden, 01062 Dresden, Germany
[b] A.E. Arbuzov Institute of Organic and Physical Chemistry, 420088 Kazan, Russia
[c] Institute of Resource Ecology, Helmholtz Centre Dresden-Rossendorf, 01314 Dresden, Germany
[d] School of Chemistry, The University of Sydney, NSW 2006, Australia

ARTICLE INFO

Article history:
Received 4 December 2014
Accepted 7 January 2015
Available online xxxx

Dedicated to Catherine Housecroft on the occasion of her 60th birthday.

Keywords:
Uranyl(VI)
Schiff base
Europium(III)
Solvent extraction
Density functional theory

ABSTRACT

The interaction of uranyl(VI) nitrate with a series of bis(2-hydroxyaryl)imine ($H_2\mathbf{L^1}$–$H_2\mathbf{L^5}$) and bis(2-hydroxyaryl)amine ($H_2\mathbf{L^8}$, $H_2\mathbf{L^9}$) derivatives incorporating 1,3-dimethylenebenzene or 1,3-dimethylenecyclohexane bridges between nitrogen sites is reported. Crystalline complexes of type $[UO_2(H_2L)(NO_3)_2]$ (where H_2L is $H_2\mathbf{L^1}$–$H_2\mathbf{L^4}$) were isolated from methanol. X-ray structures of the complexes of $H_2\mathbf{L^1}$, $H_2\mathbf{L^2}$ and $H_2\mathbf{L^4}$ show that each of these neutral ligands bind to their respective UO_2^{2+} centres in a bidentate fashion in which coordination only occurs via each ligand's hydroxy functions. Two bidentate nitrate anions complete the metal's coordination sphere in each complex to yield hexagonal bipyramidal coordination geometries. A density functional theory (DFT) investigation of $[UO_2(H_2\mathbf{L^1})(NO_3)_2]$ in a simulated methanol environment is in accord with this complex maintaining its solid state conformation in solution. Solvent extraction experiments (water/chloroform) employing $H_2\mathbf{L^1}$–$H_2\mathbf{L^7}$ in the organic phase and uranyl(VI) nitrate in the aqueous phase showed that both amine derivatives, $H_2\mathbf{L^8}$ and $H_2\mathbf{L^9}$, yielded enhanced extraction of UO_2^{2+} over the corresponding imine derivatives, $H_2\mathbf{L^1}$ and $H_2\mathbf{L^2}$. These results were further compared with those obtained for the corresponding Schiff bases incorporating 1,2-phenylene and 1,2-cyclohexane bridged ligands, $H_2\mathbf{L^6}$ and $H_2\mathbf{L^7}$; these more rigid systems also yielded enhanced extraction of UO_2^{2+} relative to the more flexible Schiff bases $H_2\mathbf{L^1}$–$H_2\mathbf{L^5}$. A very significant synergistic enhancement of the extraction of UO_2^{2+} by $H_2\mathbf{L^1}$–$H_2\mathbf{L^4}$ and $H_2\mathbf{L^7}$ was observed in the presence of a 10-fold excess of *n*-octanoic acid; the influence of pH on extraction efficiency was also investigated. A parallel set of experiments employing $H_2\mathbf{L^1}$–$H_2\mathbf{L^9}$ as extractants for europium(III) nitrate indicated a clear uptake preference for UO_2^{2+} over Eu^{3+} in all cases; separation of the uranyl ion from the rare earths is an important objective in mineral processing.

1. Introduction

The coordination chemistry of uranyl(VI) has received increasing attention over recent years [1,2]. Many such studies [3–6] were motivated by the awareness that an enhanced understanding of the complexation behaviour of this ion has implications for the winning, processing and use of uranium as well as for the appropriate control, processing and storage of nuclear wastes [7–16]. As a consequence, a number of studies have focused on ligand design for selective uranium uptake [17–20], with particular studies focused on the separation of actinides from the lanthanides [21–25] – metals which occur together in nature and nuclear wastes. However, in general, such separations are inherently challenging due to the generally similar chemistry of these ions.

In the above context it is noted that a number of Schiff base ligands have been employed for uranyl extraction [23,26,27]. For example, $H_2\mathbf{L^6}$ (salophen), has been shown to form robust neutral 1:1 uranyl chelate complexes of composition $[UO_2(\mathbf{L^6})S]$, each incorporating a solvent molecule (S = DMF, DMSO, H_2O) [28,29]. Ligand species of this type incorporating a short spacer group

* Corresponding authors. Tel.: +61 (0)2 9351 4400 (L.F. Lindoy). Tel.: +49 (0)351 463 34357 (K. Gloe).
E-mail addresses: Len.lindoy@sydney.edu.au (L.F. Lindoy), karsten.gloe@chemie.tu-dresden.de (K. Gloe).

http://dx.doi.org/10.1016/j.poly.2015.01.005
0277-5387/

(in the above case a 1,2-phenylene group) as well as structure-related species have been shown to be extracted with high efficiency into an organic phase [30]. However, bis(2-hydroxyaryl)imines, where the two terminal chelating domains are linked by extended spacer groups, have received considerably less attention even though individual examples of the latter ligands have been known for a considerable time [31].

We now report synthetic, X-ray, computational and solvent extraction studies involving the interaction of uranyl(VI) nitrate with the bis(2-hydroxyaryl)diimine derivatives ($H_2\mathbf{L^1}$–$H_2\mathbf{L^5}$) and bis(2-hydroxyaryl)diamine derivatives ($H_2\mathbf{L^8}$ and $H_2\mathbf{L^9}$), incorporating 1,3-dimethylenebenzene or 1,3-dimethylenecyclohexane units as linking backbones. The results are compared with those for the related Schiff base ($H_2\mathbf{L^6}$, $H_2\mathbf{L^7}$) ligand derivatives. Comparative results for the extraction of europium(III) with $H_2\mathbf{L^1}$–$H_2\mathbf{L^9}$ are also presented.

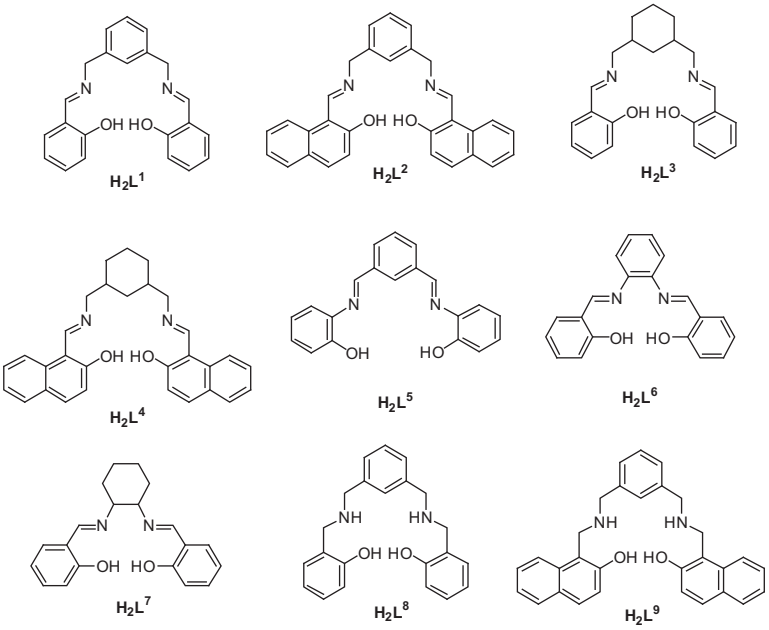

2. Experimental

2.1. Materials and instrumentation

All reagent and solvents were obtained from commercial sources and used without further purification. The ^1H and ^{13}C NMR spectra were recorded on a Bruker Avance DRX-500 spectrometer with DMSO-d^6 and $CDCl_3$ as solvents. Mass spectrometry (ESI-MS) analyses were carried out using a Bruker ESQUIRE mass spectrometer. Infrared spectra were recorded on a BioRad Excalibur FTS 3000-Spectrometer using KBr pellets. Elemental analysis (C, H, and N) were carried out on a Carlo Erba (EA 1108) Analyser. UV data were collected using a Perkin Elmer type Lambda 25 spectrophotometer in the range 200–1200 nm. The syntheses of $H_2\mathbf{L^1}$ (from m-xylylenediamine and salicylaldehyde) [32,33], $H_2\mathbf{L^5}$ (from *o*-aminophenol and isophthalaldehyde) [34], $H_2\mathbf{L^6}$ (from 1,2-phenylenediamine and salicylaldehyde) [33,35] and $H_2\mathbf{L^7}$) (from (±)-*trans*-1,2-diaminocyclohexane and salicylaldehyde) [36,37] were carried out by the respective literature procedures.

2.2. General procedure for the synthesis of Schiff base ligands $H_2\mathbf{L^2}$–$H_2\mathbf{L^4}$

A methanol solution of the required diamine and aldehyde in a 1:2 M ratio was heated under reflux for ~4 h, on cooling, to yield a yellow solid in each case which was removed by filtration. Crude $H_2\mathbf{L^3}$ was dissolved in $CHCl_3$, washed with distilled water, and the organic solvent was dried with anhydrous $MgSO_4$ and subsequently removed to obtain the pure compound. All products were washed with cold methanol, and dried under vacuum. Characterisation details are given below.

2.3. Characterisation of Schiff base ligands $H_2\mathbf{L^1}$–$H_2\mathbf{L^4}$

2.3.1. α,α′-Bis(salicylimino)-m-xylene ($H_2\mathbf{L^1}$)

From m-xylylenediamine and salicylaldehyde. Yield = 74%, ^1H NMR (500 MHz, DMSO-d_6, 25 °C, TMS): δ = 13.42 (s, 2H, OH···N), 8.72 (s, 2H, CH=N), 7.48 (dd, J = 8.6, 8.7 Hz, 2H, C_6H_4), 7.38 (t, J = 7.7, 7.5 Hz, 1H, C_6H_4), 7.35 (s, 1H, C_6H_4), 7.33 and 6.91 (t, J = 11.9, 8.2, 7.5 Hz, 4H, C_6H_4O), 7.27 (d, J = 7.6 Hz, 2H, C_6H_4O), 6.87 (d, J = 8.2 Hz, 2H, C_6H_4O), 4.82 (s, 4H, CH_2). ESI-MS (MeOH): m/z 345 [M+H$^+$]. IR (KBr pellets, cm^{-1}): ν(O—H), 3433 m (br); ν(C—H), 3054–2733w; ν(C=N),1633s; ν(C—C_{arom}), 1580–1498m. *Anal.* Calc. for $C_{22}H_{20}N_2O_2$: C, 76.72; H, 5.85; N, 8.13. Found: C, 76.78; H, 5.94; N, 8.20%.

2.3.2. α,α′-Bis(2-hydroxy-1-naphthalimino)-m-xylene ($H_2\mathbf{L^2}$)

From m-xylylenediamine and 2-hydroxy-1-naphthaldehyde. Yield, 97%. ^1H NMR (500 MHz, DMSO-d_6, 25 °C, TMS): δ = 14.38

(s, 2H, OH···N), 9.30 (d, J = 9.4 Hz, 2H, CH=N), 8.10 (d, J = 8.4 Hz, 2H, C_6H_4), 7.74 and 7.65 (d, J = 9.3, 7.9 Hz, 4H, $C_{10}H_6O$), 7.47 (s, 1H, C_6H_4), 7.40–7.46 (m, 3H, C_6H_4, $C_{10}H_6O$), 7.38 (d, J = 8.1 Hz, 2H, $C_{10}H_6O$), 7.20 (t, 2H, $C_{10}H_6O$), 6.72 (d, J = 9.3 Hz, 2H, $C_{10}H_6O$), 4.9 (d, J = 4.7 Hz, 4H, CH_2). ^{13}C NMR (500 MHz, $CDCl_3$, ppm): 174 (C—OH), 159 (CH=N), 107–138 (phenyl, naphtyl), 58 (CH_2—N). ESI-MS (MeOH): m/z 445 [M+H]. MS(ESI+) (MeOH): 445 [M+H$^+$], 889 [2M+H$^+$]. IR (KBr pellets, cm^{-1}): ν(O—H), 3434m (br); ν(C—H), 3054–2870w (sh); ν(C=N),1632s; ν(C—C_{arom}) 1544–1492w. *Anal.* Calc. for C30H24N2O2: C, 81.06; H, 5.44; N, 6.30. Found: C, 80.78; H, 5.53; N, 6.38%.

*2.3.3. α,α′-Bis(salicyliminomethyl)-1,3-cyclohexane (cis/trans) (H_2**L**^{3})*

From 1,3-bis(aminomethyl)cyclohexane and salicylaldehyde. Yield, 91%. MS(ESI+) (MeOH): 351 [M+H$^+$]. IR (KBr pellets, cm^{-1}): ν(O—H), 3434m (br); ν(C—H), 3054–2731m (ν(C=N) 1633s; ν(C—C_{arom}) 1583–1463m. *Anal.* Calc. for $C_{22}H_{26}N_2O_2$: C, 75.40; H, 7.48; N, 7.99. Found: C, 75.18; H, 7.52; N, 7.98%.

*2.3.4. α,α′-Bis(2-hydroxy-1-naphthaliminomethyl)-1,3-cyclohexane (H_2**L**^{4})*

From 1,3-bis(aminomethyl)cyclohexane and 2-hydroxy-1-naphthaldehyde. Yield, 95%. MS(ESI+) (MeOH): 451 [M+H$^+$]. IR (KBr pellets, cm^{-1}): ν(O—H), 3431m (br); ν(C—H), 3054–2852m (sh); (ν(C=N) 1630s; ν(C—C_{arom}) 1544–1449m. *Anal.* Calc. for $C_{30}H_{30}N_2O_2$ C, 79.97; H, 6.71; N, 6.22. Found: C, 80.05; H, 7.18; N, 6.25%

*2.4. Synthesis of amine ligands H_2**L**^{8} and H_2**L**^{9}*

*2.4.1. α,α′-Bis(salicylamino)-m-xylene (H_2**L**^{8})*

Slow addition of KBH4 (0.44 g, 8.2 mmol) to a stirred solution of H_2**L**^{1} (2.13 g, 6.2 mmol) in methanol (20 mL) led to isolation of crude H_2**L**^{8} as an oily material which was dissolved in a small volume of chloroform and the solution shaken with water. The chloroform phase was separated, dried over anhydrous $MgSO_4$, then the solvent removed to yield the product as a viscous yellow–brown oil (1.50 g, 70%). ^1H NMR (500 MHz, $CDCl_3$, 25 °C, TMS): δ = 7.32 (t, J = 7.3 Hz, 1H, C_6H_4), 7.24 (s, 2H, OH), 7.23 (s, 1H, C_6H_4), 7.22 (d, J = 7.5 Hz, 2H, C_6H_4O), 7.16 (t, J = 1.6, 1.1 Hz, 2H, C_6H_4O), 6.97 (d, J = 1.1 Hz 2H, C_6H_4O), 6.84 (d, J = 0.9 Hz, 2H, C_6H_4), 6.77 (t, J = 1.1, 1.0 Hz, 2H, C_6H_4O), 5.28 (s, 2H, NH), 4.00 (s, 4H, CH_2—N), 3.80 (s, 4H, CH_2)MS(ESI+) (MeOH): 349 [M+H$^+$]. *Anal.* Calc. for $C_{22}H_{24}N_2O_2$: C, 75.83; H, 6.94; N, 8.04. Found: C, 75.90; H, 6.98; N, 8.15%.

*2.4.2. α,α′-Bis(2-hydroxy-1-naphthalamino)-m-xylene (H_2**L**^{9})*

Using a similar procedure to that employed for H_2**L**^{8} but starting with H_2**L**^{2} gave H_2**L**^{9} as a viscous yellow–brown oil (1.65 g, 85%). ^1H NMR (500 MHz, $CDCl_3$, 25 °C, TMS): δ = 7.62 (t, J = 8.3 Hz, 1H, C_6H_4), 7.54 (s, 2H, OH), 7.53 (s, 1H, C_6H_4), 7.51 (d, J = 6.5 Hz, 2H, $C_{10}H_6O$), 7.46 (d, J = 7.5 Hz, 2H, $C_{10}H_6O$), 7.32 (t, J = 1.3 Hz 2H, $C_{10}H_6O$), 7.23 (d, J = 0.9 Hz, 2H, $C_{10}H_6O$), 7.20 (t, J = 1.8 Hz, 2H, $C_{10}H_6O$), 7.12 (d, J = 6.2 Hz, 2H, $C_{10}H_6O$), 5.28 (s, 2H, H_{NH}), 4.72 (s, 4H, CH_2—N), 3.9 (s, 4H, CH_2). MS(ESI+) (MeOH): 449 [M+H$^+$]. *Anal.* Calc. for $C_{27}H_{24}N_2O_2$: C, 80.33; H, 6.29; N, 6.25. Found: C, 80.10; H, 6.37; N, 6.31%.

2.5. Synthesis of uranyl(VI) complexes

*2.5.1. General procedure for the synthesis of **1**–**4***

Complexes **1**–**4** of type $[UO_2(H_2L)(NO_3)_2]$ (H_2L = H_2**L**^{1}–H_2**L**^{4}) were synthesized by heating the required Schiff base ligand (1 mmol) and $UO_2(NO_3)_2{\cdot}6H_2O$ (1 mmol) at the reflux temperature for 12 h in methanol. The resulting orange–red precipitates were filtered, washed with cold methanol, and dried under vacuum. Characterisation details are given below. Crystals of **1**, **2** and **4** suitable for X-ray diffraction were obtained by slow diffusion of diethylether into an equimolar methanol/acetonitrile (1:1) (1 mL) solution of the complex over one week. The crystals were collected, washed with ether, and dried under vacuum.

*2.5.2. Characterisation of uranyl(VI) complexes (**1**)–(**4**)*

*2.5.2.1. $[UO_2(H_2L^1)(NO_3)_2]$ (**1**).* Yield, 89%. MS(ESI+) (MeOH): 613 [$UO_2(H_2$**L**^{1}) – H$^+$], 676 [UO_2(**L**^{1})$(NO_3)]^+$. UV/Vis (MeOH): 324 (ε = 17 000), 357 (ε = 18 600) nm. ^1H NMR (500 MHz, DMSO-d_6, 25 °C, TMS): δ [ppm] = 13.01 (s, 2H, OH···N), 8.83 (s, 2H, CH=N), 7.48 (dd, J = 7.6 Hz, 2H, C_6H_4), 7.39 (t, J = 7.6, 7.5 Hz, 1H, C_6H_4), 7.35 (s, 1H, C_6H_4), 7.33 and 6.91 (t, J = 11.2, 7.5 Hz, 4H, C_6H_4O), 7.28 (d, J = 7.7 Hz, 2H, C_6H_4O), 6.87 (d, J = 8.3 Hz, 2H, C_6H_4O), 4.82 (s, 2H, CH_2). IR (KBr): 3433m, 3158m, 3066w, 2427w, 1651s, 921s cm^{-1}. *Anal.* Calc. for $C_{22}H_{20}N_4O_{10}U$: C, 35.78; H, 2.73; N, 7.59. Found: C, 35.38; H, 3.00; N, 7.50%.

*2.5.2.2. $[UO_2(H_2L^2)(NO_3)_2]$ (**2**).* Yield, 94%. MS(ESI+) (MeOH): 713 [$UO_2(H_2$**L**^{2}) – H$^+$]. UV–Vis (MeOH): 310 (ε = 13 200), 334 (ε = 13 200), 398 (ε = 14 800), 420 (ε = 12 000) nm. ^1H NMR (500 MHz, DMSO-d_6, 25 °C, TMS): δ [ppm] = 13.99 (s, 2H, OH···N), 9.39 (d, J = 14.9 Hz, 2H, CH=N), 8.15 (dd, J = 11.5, 12 Hz, 2H, C_6H_4), 7.82 and 7.70 (d, J = 9.6, 7.3 Hz, 4H, $C_{10}H_6O$), 7.40–7.48 (m, 4H, C_6H_4, $C_{10}H_6O$), 7.38 (d, J = 8.6 Hz, 2H, $C_{10}H_6O$), 7.25 (t, 2H, $C_{10}H_6O$), 6.81 (d, J = 7.3 Hz, 2H, $C_{10}H_6O$), 4.94 (d, J = 9.7 Hz, 4H, CH_2). IR (KBr): 3430m, 3067w, 2926w, 2427w, 1638s, 921m cm^{-1}. *Anal.* Calc. for $C_{30}H_{24}N_4O_{10}U$: C, 42.97; H, 2.88; N, 6.68. Found: C, 42.52; H, 2.98; N, 6.97%.

*2.5.2.3. $[UO_2(H_2L^3)(NO_3)_2]$ (**3**).* Yield, 76%. MS(ESI+) (MeOH): 619 [$UO_2(H_2$**L**^{3}) – H$^+$], 679 [UO_2(**L**^{3})$(NO_3)]^+$ UV–Vis (MeOH): 322 (ε = 4000), 376 (ε = 5200) nm. IR (KBr): 3433m, 3062w, 2925m, 2856w, 2427w, 1654s, 920s cm^{-1}. *Anal.* Calc. for $C_{22}H_{26}N_4O_{10}U$: C, 35.49; H, 3.52; N, 7.53. Found: C, 35.05; H, 3.63; N, 7.57%.

*2.5.2.4. $[UO_2(H_2L^4)(NO_3)_2]$ (**4**).* Yield, 90%. MS(ESI+) (MeOH): 719 [$UO_2(H_2$**L**^{4}) – H$^+$], 782 [UO_2(**L**^{13})$(NO_3)]^+$. UV–Vis (MeOH): 338 (ε = 15 400), 395 (ε = 13 600), 418 (ε = 10 600) nm. IR (KBr): 3428m, 3065w, 2926w, 2853w, 2427w, 1640s, 921s cm^{-1}; *Anal.* Calc. for $C_{30}H_{30}N_4O_{10}U$: C, 42.66; H, 3.58; N, 6.63. Found: C, 42.67; H, 3.76; N, 6.60%.

2.6. X-ray data collection and structure solution

X-ray diffraction data for $[UO_2(H_2$**L**$^1)(NO_3)_2]$ (**1**) was collected on a Nonius Kappa CCD with ω and φ scans at 293(2) K. Data collections were undertaken with COLLECT [38], cell refinement with Dirax/lsq [39], and data reduction with EvalCCD [40]. Data for structures $[UO_2(H_2$**L**$^2)(NO_3)_2]$ (**2**) and $[UO_2(H_2$**L**$^4)(NO_3)_2]$ (**4**) were collected at 160(2) and 198(2) K respectively using a Bruker AXS Kappa APEX II CCD diffractometer with an Oxford Cryosystems coldhead attached. Data integration and reduction were undertaken with SAINT and APEX2 [41–43]. Each structure was solved by direct methods using SHELXS-97 [43] employing graphite-monochromated Mo Kα radiation (0.71073 Å) generated from a sealed tube. Multi-scan empirical absorption corrections were applied to all data sets using SADABS [44]. All structures were refined and extended with SHELXL-97 [45]. In general, ordered non-hydrogen atoms with occupancies greater than 0.5 were refined anisotropically. Partial occupancy carbon, nitrogen and oxygen atoms were refined isotropically. Carbon-bound hydrogen atoms were included in idealised positions and refined using a riding model. Oxygen and nitrogen bound hydrogen atoms that were structurally evident in the difference Fourier map were included and refined

Table 1
Crystal data and structure refinement details of **1**, **2**, and **4**.

Compound	$[UO_2(H_2\mathbf{L}^1)(NO_3)_2]$ (**1**)	$[UO_2(H_2\mathbf{L}^2)(NO_3)_2]$ (**2**)	$[UO_2(H_2\mathbf{L}^4)(NO_3)_2]$ (**4**)
Molecular formula	$C_{22}H_{20}N_4O_{10}U$	$C_{30}H_{24}N_4O_{10}U$	$C_{30}H_{30}N_4O_{10}U$
Mr	738.45	838.56	844.61
Crystal system	triclinic	monoclinic	triclinic
Space group	$P\bar{1}$	$C2/c$	$P\bar{1}$
a (Å)	9.471 (1)	31.190 (6)	11.107 (1)
b (Å)	9.510 (1)	11.082 (2)	11.424 (3)
c (Å)	15.251 (2)	17.951 (4)	13.060 (2)
α (°)	72.17 (1)	90	112.12 (2)
β (°)	89.36 (1)	113.32 (3)	90.058 (10)
γ (°)	70.70 (1)	90	101.066 (10)
V (Å^3)	1228 (3)	5698 (2)	1501.7 (5)
D_{calc} (g cm^{-3})	1.997	1.955	1.859
Z	2	8	2
Crystal size (mm)	0.38 × 0.28 × 0.19	0.14 × 0.11 × 0.03	0.15 × 0.07 × 0.04
Crystal colour	orange–red	orange–red	orange–red
Crystal habit	polyhedron	polyhedron	polyhedron
T (K)	293(2)	160(2)	198(2)
λ (Mo Kα)	0.71073	0.71073	0.71073
μ (Mo Kα) (mm^{-1})	6.673	5.765	5.47
$2\theta_{max}$ (°)	60	54	54
N	67317	31794	50574
N_{ind} (R_{merge})	7136 (0.040)	6059 (0.075)	6550 (0.066)
N_{obs} – ($I > 2\sigma(I)$)	7136	6059	5640
R_1[a] – ($I > 2\sigma(I)$)	0.021	0.027	0.032
wR_2[a] – (all)	0.049	0.048	0.060
Resid. Extr. (e$^-$ Å^{-3})	1.32 (−1.23)	0.79 (−0.83)	1.16 (−1.08)

[a] $R_1 = \sum||F_o| - |F_c||/\sum|F_o|$ for $F_o > 2r(F_o)$ and $wR_2 = \{\sum[w(F_o^2 - F_c^2)^2]/\sum[w(F_c^2)^2]\}^{1/2}$ where $w = 1/[\sigma^2(F_o^2) + (AP)^2 + BP]$, $P = (F_o^2 + 2F_c^2)/3$ and A and B are listed in the crystal data information supplied.

with bond length and angle restraints. Crystal and structure refinement data for all three structures are summarised in Table 1.

2.7. DFT calculations

Density functional theory (DFT) calculations were carried out to optimize the structure of $[UO_2(H_2\mathbf{L}^1)(NO_3)_2]$ (**1**) in methanol, as well as to compare the stability of an alternative isomeric arrangement. Geometry optimization and Gibbs energy calculations were performed at the B3LYP level using CPCM [46] with UAHF radii [47] using the program package Gaussian 03 [48]. Small core effective core potentials (ECPs) were used on U, O, C, and N atoms with the corresponding basis sets [49]. For hydrogen, the 5s functions contracted to 3s were employed [50].

2.8. Solvent extraction experiments

The solvent extraction experiments were performed at 23 ± 1 °C in microcentrifuge tubes (2 mL) with a phase ratio $V_{(w)}$:$V_{(org)}$ of 1:1 (0.5 mL each). The aqueous phase contained 1×10^{-4} M $UO_2(NO_3)_2$, and a zwitterionic buffer system (MES/NaOH at pH 5.2 or HEPES/NaOH at pH 7.2); as a precaution, the pH of the aqueous phase was monitored before and after each experiment with the aid of an InLab423 pH electrode. Constant ionic strength was maintained in the aqueous phase by the addition of $NaNO_3$ (5×10^{-3} M). The $CHCl_3$ phase contained a known concentration of ligand (1×10^{-2} M) and in particular cases also *n*-octanoic acid (1×10^{-3} M). The extraction experiments involved mechanical shaking of the two-phase system for 1 h. ($T = 23 \pm 1$ °C) during which time equilibrium was established (the time to reach equilibrium was established by preliminary experiments). The phases were then separated, centrifuged and duplicate 100 µL samples removed for analysis. The depletion of the uranyl ion concentration in the respective aqueous phases was measured using an ICP-MS (ELAN 9000/Perkin Elmer) spectrometer. Except for low extraction values which are subject to higher error, an overall error of approximately ±5% applies to the remaining extractions. The concentrations of Eu(III) were measured in both phases radiometrically using ^{152}Eu (ROTOP Pharmaka) by means of a NaI(Tl) scintillation counter (Cobra II/ Canberra-Packard) [51].

3. Results and discussion

3.1. Ligand and complex synthesis

All Schiff base ligands were obtained as yellow solids by the usual procedure [52,53] of heating the required diamine and aldehyde derivatives in a 1: 2 M ratio in methanol or ethanol. Reduction of $H_2\mathbf{L}^1$ and $H_2\mathbf{L}^2$ to give $H_2\mathbf{L}^8$ and $H_2\mathbf{L}^9$ was achieved by treating the respective Schiff bases in methanol with KBH_4.

The uranyl(VI) complexes $[UO_2(H_2\mathbf{L}^1)(NO_3)_2]$ (**1**), $[UO_2(H_2\mathbf{L}^2)(NO_3)_2]$ (**2**), $[UO_2(H_2\mathbf{L}^3)(NO_3)_2]$ (**3**) and $[UO_2(H_2\mathbf{L}^4)(NO_3)_2]$ (**4**) were synthesised by heating equimolar amounts of $UO_2(NO_3)_2$ and the required ligand in methanol. Microanalytical and ESI-MS data were consistent with the above formulation of the respective products incorporating the non-deprotonated forms of $H_2\mathbf{L}^1$–$H_2\mathbf{L}^4$. Comparison of the ^{1}H NMR spectra of individual free ligands and their complexes indicated little shift in the respective CH_{imine} proton signal in accord with non-coordination of the imine functions in **1**–**4**. A small upfield shift of about 0.45 ppm for the phenolic group in all the complexes relative to the corresponding free ligands is in keeping with coordination of the phenolic oxygen with the UO_2 centre in each case. Similarly, a strong peak at or near 1645 cm^{-1} in their infrared spectra (versus ~1632 cm^{-1} for the free ligands) [54] is in keeping with a significant interaction of the imine nitrogen with the hydrogen of the hydroxyl group; a new (weak) peak at ~2427 cm^{-1} is assigned to the ν(CH═N···H) vibration. Further, evidence for coordination of the phenolic hydroxyl group is given by a peak at 1350 cm^{-1} assigned to $\nu(C_{arom}$—O) for each of **1**–**4** – shifted from 1385–1384 cm^{-1} in the spectra of the corresponding free ligands. All complexes displayed strong bands at ~920 cm^{-1} assigned to the νUO_{2asym} stretch [55,56].

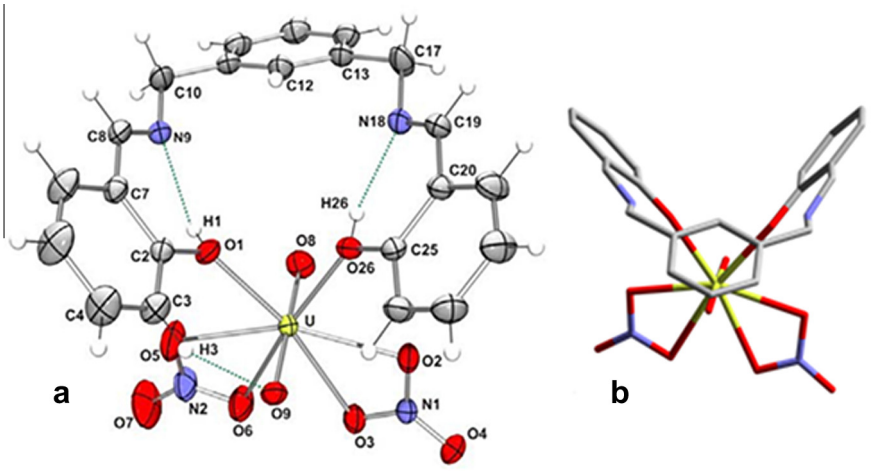

Fig. 1. (a) X-ray structure of $[UO_2(H_2\mathbf{L}^1)(NO_3)_2]$ (**1**) showing the all-oxygen coordination sphere of the U(VI) ion. Thermal ellipsoids are shown at the 30% probability level. (b) View illustrating the configuration adopted by the bound $H_2\mathbf{L}^1$ and the bidentate nitrato ligands around the UO_2^{2+} centre.

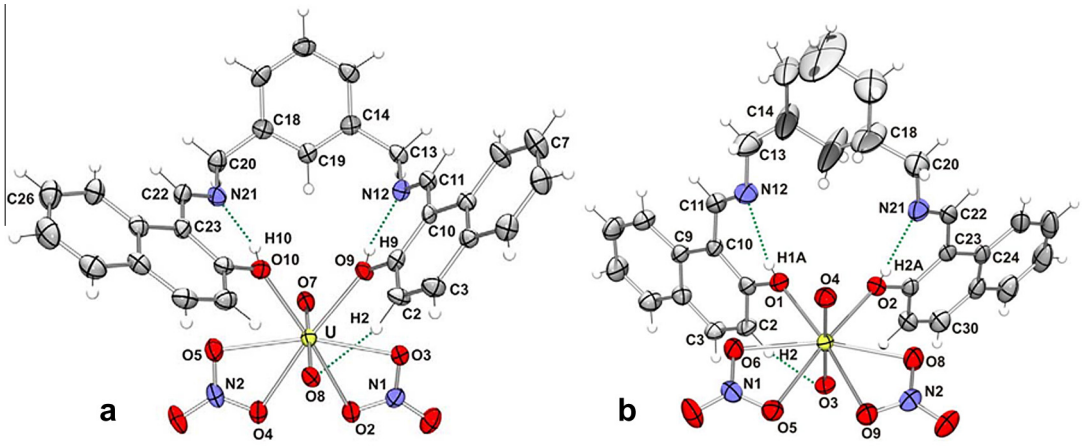

Fig. 2. X-ray structure of (a) $[UO_2(H_2\mathbf{L}^2)(NO_3)_2]$ (**2**) with thermal ellipsoids shown at the 30% probability level and (b) $[UO_2(H_2\mathbf{L}^4)(NO_3)_2]$ (**4**) with thermal ellipsoids shown at the 50% probability level.

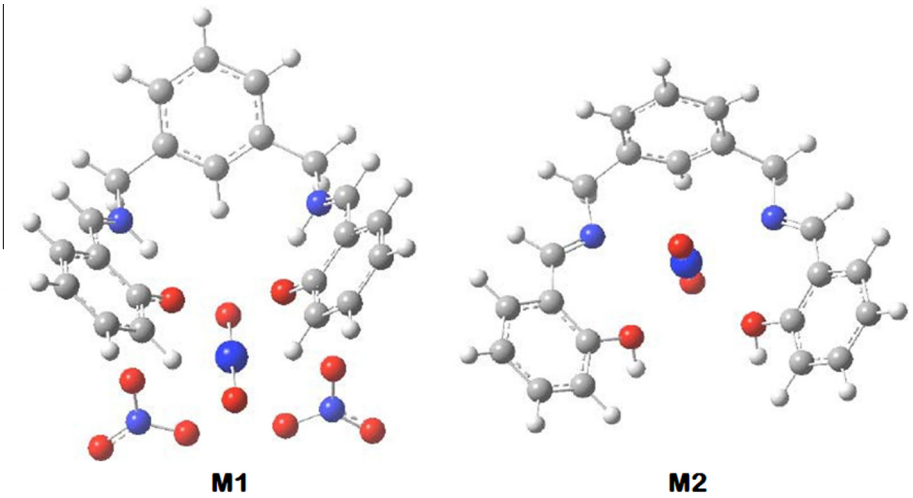

Fig. 3. Calculated structures of two uranyl(VI) complexes (**M1**, **M2**) of the neutral Schiff base ligand $H_2\mathbf{L}^1$ optimized for solution in CH_3OH at the B3LYP level.

Table 2
Selected bond lengths [Å] and angles [°] for **1**, **2** and **4**.

*[$UO_2(H_2L^1)(NO_3)_2$] (**1**)*			
U–O(8)	1.760(2)	U–O(1)	2.324(1)
U–O(9)	1.763(2)	U–O(26)	2.311(2)
U–O(2)	2.519(2)	U–O(5)	2.579(3)
U–O(3)	2.575(2)	U–O(6)	2.596(3)
O(8)–U–O(9)	178.09(11)	O(1)–U–O(26)	75.49(9)
O(1)–U–O(8)	90.19(9)	O(26)–U–O(8)	85.91(10)
O(1)–U–O(9)	90.64(8)	O(26)–U–O(9)	95.96(8)
O(2)–U–O(3)	49.25(7)	O(5)–U–O(6)	48.02(11)
*[$UO_2(H_2L^2)(NO_3)_2$] (**2**)*			
U–O(7)	1.750(3)	U–O(10)	2.358(3)
U–O(8)	1.739(4)	U–O(9)	2.345(3)
U–O(2)	2.504(3)	U–O(4)	2.519(4)
U–O(3)	2.544(3)	U–O(5)	2.547(4)
O(7)–U–O(8)	178.63(17)	O(9)–U–O(10)	71.27(12)
O(10)–U–O(7)	88.69(13)	O(9)–U–O(7)	86.77(14)
O(10)–U–O(8)	91.74(13)	O(9)–U–O(8)	94.60(15)
O(2)–U–O(3)	50.32(11)	O(4)–U–O(5)	50.3(11)
*[$UO_2(H_2L^4)(NO_3)_2$] (**4**)*			
U–O(3)	1.765(3)	U–O(2)	2.335(2)
U–O(4)	1.763(3)	U–O(1)	2.385(3)
U–O(5)	2.570(3)	U–O(8)	2.509(3)
U–O(6)	2.546(3)	U–O(9)	2.534(3)
O(3)–U–O(4)	179.34(13)	O(1)–U–O(2)	71.63(9)
O(2)–U–O(3)	93.34(11)	O(1)–U–O(3)	92.30(12)
O(2)–U–O(4)	86.73(14)	O(1)–U–O(4)	88.34(12)
O(5)–U–O(6)	49.48(9)	O(8)–U–O(9)	50.16(11)

3.2. X-ray structures

Orange–red crystals of **1**, **2** and **4** of type $[UO_2(H_2L)(NO_3)_2]$ that were suitable for X-ray diffraction studies were obtained by slow diffusion of diethyl ether into a methanol/acetonitrile solution of the respective complexes. The asymmetric unit of each complex contains one U(VI) ion, one ligand molecule and two nitrate anions. The coordination geometries present in all three complexes (Figs. 1–3) are quite similar, with each complex showing a distorted hexagonal-bipyramidal arrangement about its U(VI) centre, with an axially oriented O=U=O moiety and six equatorial oxygen atoms. In all three structures the aryl and naphthyl groups are present on the same side of the equatorial plane [see, for example Fig. 1(b)].

The U=O distances and O=U=O angles in **1** (av. 1.76(2) Å; 178°), **2** (av. 1.75(4) Å; 179°) and **4** (av. 1.76(3) Å; 179°) are typical of the corresponding distances and angles reported for related uranyl compounds [26,28,30,57].

As suggested by the physical data, the X-ray diffraction studies in each case confirm that the uranyl ion is bound to the phenolic OH groups of the respective neutral ligands ($H_2\mathbf{L^1}$, $H_2\mathbf{L^2}$ and $H_2\mathbf{L^4}$) and two bidentate nitrate ions. The U—O_{phenol} bond lengths appear unremarkable for each of **1** (2.311 and 2.324 Å), **2** (2.345 and 2.358 Å) and **4** (2.333 and 2.341 Å), being slightly longer than the distances (2.202–2.298 Å) observed in related uranyl(VI) salicylideneimine complexes in which the coordinated phenolic group is deprotonated [26,28,30,58]. The U—$O_{nitrate}$ bonds are longer at 2.519–2.596 Å (**1**), 2.504–2.547 Å (**2**), 2.509–2.570 Å (**4**). The imine nitrogens do not bind to the UO_2^{2+} cation, but in each case are associated with an intramolecular hydrogen bond (O—H···N=C) with the nearest phenolic hydroxy function [59]; the bond distances are (1.98 and 1.94 Å), (1.81 and 1.85 Å) and (1.88 and 1.99 Å) for **1**, **2**, and **4** respectively [shown as dotted lines in Figs. 1–3]. Large thermal displacements of the C atoms in the central cyclohexyl ring in **4** were found and the ring was hence modelled as positionally disordered over two sites. However, for the sake of clarity, only one position is shown in Fig. 2(b).

All three complexes represent new examples of the rare U(VI) complex category incorporating bound neutral hydroxyaryl Schiff base ligands [31]. Selected bond distances and angles are listed in Table 2.

The crystal packing in all three products is characterised by extended networks of weak interactions that include hydrogen bonds, π–π and CH-π interactions between ligand molecules, the uranyl group and nitrate anions. Individual nitrate oxygen atoms are involved in hydrogen bonds that bridge to adjacent molecules through hydrogen bond interactions that fall in the ranges 2.44–2.60 Å (**1**), 2.35–2.58 Å (**2**), 2.59–2.60 Å (**4**) (see also the Supporting information). Also, in each structure weak intramolecular hydrogen bond interactions are present between one of the uranyl oxygens and an adjacent aromatic C—H group; the C—H···O=U (C···O) distances are 3.20 Å, 3.30 Å and 3.23 Å in **1**, **2** and **4** respectively. In each structure, stacking of the complex molecules occur via π–π [3.64 Å(1), 3.76–3.79 Å(2), 3.61–3.79 Å(4)] and CH-π [2.61–3.05 Å (**1**), 2.70–2.92 Å (**2**), 2.83–2.96 Å (**4**)] interactions. Further structural details and packing diagrams for **1**, **2** and **4** are presented in the Supplementary data.

3.3. DFT computational study

A DFT investigation of $[UO_2(H_2\mathbf{L^1})(NO_3)_2]$ (**1**) in a simulated methanol environment was performed in order to probe the structure of the complex in this solvent. Comparative DFT modelling of the corresponding hypothetical complex in which the UO_2^{2+} group binds to the O_2N_2-donor set of the neutral ligand (nitrates not coordinated) was also carried out. The results are shown in Fig. 3. The optimised structure (**M1**) based on the crystal structure of **1** is quite close to that observed in the crystal with, in particular, the confirmation of $\mathbf{L^1}$ essentially maintaining the conformation observed in the solid state. For **M2**, the structure incorporating UO_2^{2+} ion bound to all four (O_2N_2) donor atoms of $\mathbf{L^1}$, there is a substantial change in the conformation of bound $H_2\mathbf{L^1}$. In particular, the backbone 1,3-phenylene ring is rotated significantly further from the mean O_2N_2-donor plane of $\mathbf{L^1}$ in order to minimise a steric clash (in the absence of proton loss) [60] that otherwise would occur between the hydrogen in the 2-position of the ring and the introduced uranyl(VI) ion if the ligand conformation observed in **M1** was maintained. It is proposed that this steric interference plays a major role in destabilising structure **M2** relative to **M1**.

The calculations also confirm the presence of strong OH···N interactions between adjacent sites on each salicylimine moiety

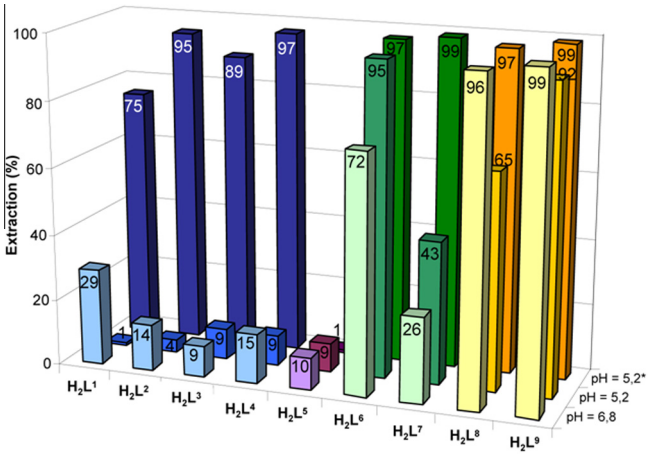

Fig. 4. UO_2^{2+} extraction by $H_2\mathbf{L^1}$–$H_2\mathbf{L^9}$ at pH 5.2 and 6.8 as well as in the presence of *n*-octanoic acid at pH 5.2(*); [U(VI)] = 1×10^{-4} M, [$NaNO_3$] = 5×10^{-3} M; [L] = 1×10^{-2} M, *[*n*-octanoic acid] = 1×10^{-3} M in $CHCl_3$; t = 60 min, T = 23 ± 1 °C.

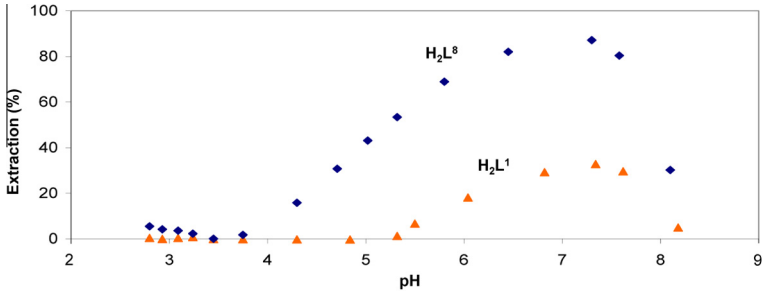

Fig. 5. The pH dependence of UO_2^{2+} extraction with the ligands $H_2\mathbf{L}^1$ and $H_2\mathbf{L}^8$. The downturn in extraction at pH values above ~7 is almost certainly reflects the occurrence of metal hydrolysis in the aqueous phase.

Table 3
Comparison of selected bond lengths [Å] for **1** obtained from the DFT study with those obtained from the X-ray diffraction determination.

	M1 (calcd.)	**1** (X-ray)
$U–O_{axial}$	1.776, 1.782	1.760(2), 1.763(2)
$U–O_{nitrate}$	2.611, 2.615	2.519(2), 2.579(3)
	2.613, 2.615	2.579(3), 2.596(3)
$U–O_{phenolic}$	2.322, 2.324	2.324(1), 2.311(2)

of metal-bound $H_2\mathbf{L}^1$. Comparison of the calculated coordination bond lengths for $[UO_2(H_2\mathbf{L}^1)(NO_3)_2]$ (**M1**) in methanol obtained by DFT are in good agreement with the corresponding X-ray data obtained for $[UO_2(H_2\mathbf{L}^1)(NO_3)_2]$ (**1**) (Table 3).

4. Solvent extraction studies

The extraction of U(VI) and Eu(III) using $H_2\mathbf{L}^1$–-$H_2\mathbf{L}^9$ involved parallel sets of experiments in both the absence and presence of *n*-octanoic acid; the results for UO_2^{2+} are summarised in Fig. 4. The lipophilicities of the Schiff base ligands in the above series are similar as shown by measuring their distribution between water and *n*-octanol. In general, the extraction efficiency of the Schiff bases $H_2\mathbf{L}^1$–-$H_2\mathbf{L}^5$ for U(VI) is quite limited [at pH 5.2 only 1–9% of the U(VI) in the aqueous phase was extracted] but this was somewhat increased with rising pH (at pH 6.8 the extraction lies between 9 and 29%).

Of all the Schiff bases studied (that is, $H_2\mathbf{L}^1$–$H_2\mathbf{L}^7$) only $H_2\mathbf{L}^6$ (95%) and the analogous 1,2-cyclohexane linked ligand $H_2\mathbf{L}^7$ (43%) exhibited substantial extraction efficiencies at pH 5.2. This significantly enhanced extraction by $H_2\mathbf{L}^6$ and $H_2\mathbf{L}^7$ undoubtedly reflects that, relative to the other Schiff base ligands in the series, both these ligands are capable of yielding stable neutral chelate ring patterns with N_2O_2-donor coordination on 1:1 complexation with UO_2^{2+}. This behaviour contrasts with the preferred O_2-donor coordination of $H_2\mathbf{L}^1$–$H_2\mathbf{L}^4$ (along with the binding of two nitrate anions).

As expected, the related secondary amine ligands $H_2\mathbf{L}^8$ (65% extraction) and $H_2\mathbf{L}^9$ (92% extraction) give rise to higher extraction efficiencies relative to the Schiff bases. This observation is in accord with both the consequence of the greater flexibility of their backbone structures and the higher basicities of these amine derivatives. Furthermore, the higher extraction efficiency of $H_2\mathbf{L}^9$ relative to $H_2\mathbf{L}^8$ is in accord with the former's enhanced lipophilicity.

Addition of ten equivalents (relative to the metal ion concentration) of *n*-octanoic acid to the organic phase resulted in the extraction of UO_2^{2+} by $H_2\mathbf{L}^1$–$H_2\mathbf{L}^4$ being markedly enhanced at pH 5.2 (from a few percent to >75% extraction) reflecting a remarkably large synergistic effect in each case; no extraction (⩽1%) was observed with the acid alone under comparable conditions. Only the extraction by $H_2\mathbf{L}^5$ (possessing different relative positions of its two imine function in comparison to the other ligands) is not influenced by addition of the above acid. Under comparable conditions Eu(III) extraction with all ligands was negligible (⩽1%). Clearly the extraction efficiency of these ligands strongly favours U(VI) over Eu(III) both in the absence and in the presence of *n*-octanoic acid.

The influence of the pH of the aqueous phase on extraction has been investigated. A significant increase of extraction with rising pH was found especially for the amine-containing ligands $H_2\mathbf{L}^8$ and $H_2\mathbf{L}^9$. For the latter ligands, this observation is in accord with both the greater flexibility of their backbone structures and the higher basicity of these amine-containing derivatives. Furthermore, the higher extraction efficiency of $H_2\mathbf{L}^9$ relative to $H_2\mathbf{L}^8$ is in accord with the former's higher lipophilicity.

The pH dependence of UO_2^{2+} extraction by the Schiff base $H_2\mathbf{L}^1$ and the structure-related secondary amine ligand $H_2\mathbf{L}^8$ is illustrated in Fig. 5. In accord with the above, for a given pH the extraction efficiency of the latter ligand is substantially higher. Related pH dependence studies for $H_2\mathbf{L}^3$–$H_2\mathbf{L}^4$ also indicated that the highest extraction is achieved at pH ~7; the respective values (at pH 6.8) are shown in Fig. 4.

The increased extraction on rising the pH of the aqueous phase is in accord with the deprotonation of the phenolic OH functions of the ligands occurring as the pH is increased, ultimately resulting in the formation of neutral uranyl complexes; however, it is noted that a "slope analysis" [51] involving a log D versus pH plot, where D is the distribution ratio for UO_2^{2+} between the aqueous and organic phase at equilibrium, did not correspond to the expected release of two protons – in keeping with the presence of competing equilibria rather than simple 1:1 complex behaviour (with loss of two protons) occurring in the organic phase.

5. Conclusion

Unusual uranyl complexes of neutral phenolic Schiff base ligands have been synthesised and characterised by a range of physical methods that includes X-ray crystallography. These complexes do not use their imine functions for binding to the UO_2^{2+}, an outcome attributed to steric hindrance from the proton in the 2-position of the phenylene ring in the backbone bridging unit. The extraction properties of the ligands $H_2\mathbf{L}^1$–$H_2\mathbf{L}^5$ towards U(VI) are quite similar. However, the distribution ratios of UO_2^{2+} with these 1,3-phenylene bridged derivatives are significantly lower than in case of the related 1,2-bridged compounds $H_2\mathbf{L}^6$ and $H_2\mathbf{L}^7$ which almost certainly use their O_2N_2 donor sets for binding the uranyl ion (coupled with concomitant loss of both their phenol protons). The preference of the 1,3-linked bis(2-hydroxyaryl)imine species $H_2\mathbf{L}^1$–$H_2\mathbf{L}^4$ to act as neutral ligands towards UO_2^{2+} in such complexes in conjunction with nitrato ligands provides a rationale for the strong synergistic effect observed in the presence of *n*-octanoic acid (at pH 5.2). That is, the hydrophobic carboxylate anion likely replaces the nitrato ligands in the coordination sphere leading to a higher complex

lipophilicity and, consequently, improved extraction efficiency. Finally, all ligands studied favour the extraction of U(VI) over Eu(III) – an outcome that points the way towards their possible use in rare earth/uranium separation processes.

Acknowledgements

The authors thank the German Federal Ministry of Education and Research (BMBF – project 02NUK014A) and the European Research Council (ERC) (SynPhosproject number 307616) for financial support. J. Mizera gratefully acknowledges the European Social Fund for a Ph.D. grant.

Appendix A. Supplementary data

CCDC 1036931, 1036932 and 1036930 contain the supplementary crystallographic data for the complexes **1**, **2** and **4** respectively. These data can be obtained free of charge via http://www.ccdc.cam.ac.uk/conts/retrieving.html, or from the Cambridge Crystallographic Data Centre, 12 Union Road, Cambridge CB2 1EZ, UK; fax: (+44) 1223-336-033; or e-mail: deposit@ccdc.cam.ac.uk. Supplementary data associated with this article can be found, in the online version, at http://dx.doi.org/10.1016/j.poly.2015.01.005.

References

[1] (a) See, for example: I.T. Ho, Z. Zhang, M. Ishida, V.M. Lynch, W.Y. Cha, Y.M. Sung, D. Kim, J.L. Sessler, J. Am. Chem. Soc. 136 (2014) 4281;
(b) Z. Asadi, F. Golzard, V. Eigner, M. Dusek, J. Coord. Chem. 66 (2013) 3629;
(c) P.L. Arnold, G.M. Jones, Q.-J. Pan, G. Schreckenbach, J.B. Love, Dalton Trans. 41 (2012) 6595;
(d) G.M. Lombardo, A.L. Thompson, F.P. Ballistreri, A. Pappalardo, G.T. Sfrazzetto, G.A. Tomaselli, R.M. Toscano, F. Punzo, Dalton Trans. 41 (2012) 1951;
(e) Q.J. Pan, S.O. Odoh, G. Schreckenbach, P.L. Arnold, J.B. Love, Dalton Trans. 41 (2012) 8878;
(f) K. Takao, M. Kato, S. Takao, A. Nagasawa, G. Bernhard, C. Hennig, Y. Ikeda, Inorg. Chem. 49 (2010) 2349;
(g) J.B. Love, Chem. Commun. (2009) 3154;
(h) H Naeimi, F. Salimi, K. Rabiei, J. Coord. Chem. 61 (2008) 3659;
(i) M.S. Bharara, S.A. Tonks, A.E.V. Gorden, Chem. Commun. (2007) 4006
[2] V. Rericha, M. Kulich, R. Rericha, D.L. Shore, D.P. Sandler, Environ. Health Perspect. 114 (2006) 818.
[3] T.W. Hayton, J.M. Boncella, B.L. Scott, E.R. Batista, P.J. Hay, J. Am. Chem. Soc. 128 (2006) 10549.
[4] M. Sawicki, J.M. Siaugue, C. Jacopin, C. Moulin, T. Bailly, R. Burgada, S. Meunier, P. Baret, J.L. Pierre, F. Taran, Chem. Eur. J. 11 (2009) 3689.
[5] I. Castro-Rodriguez, K. Olsen, P. Gantzel, K. Meyer, J. Am. Chem. Soc. 125 (2003) 4565.
[6] A.E.V. Gorden, J.D. Xu, K.N. Raymond, P. Durbin, Chem. Rev. 103 (2003) 4207.
[7] J.M. Hashke, J.L. Stakebake, in: L.R. Morss, N.M. Edelstein, J. Fuger (Eds.), The Chemistry of the Actinide and Transactinide Elements, Springer, 2006, p. 3199 (Chapter 29).
[8] G.R. Choppin, J. Radioanal. Nucl. Chem. 273 (2007) 695.
[9] G.R. Choppin, M.P. Jensen, in: L.R. Morss, N.M. Edelstein, J. Fuger (Eds.), The Chemistry of the Actinide and Transactinide Elements, Springer, 2006, p. 2554 (Chapter 23).
[10] S.H. Thomas, E. Padilla-Crespo, P.M. Jardine, R.A. Sanford, F.E. Loffler, Appl. Environ. Microbiol. 75 (2009) 3679.
[11] T. Mathews, K. Beaugelin-Seiller, J. Garnier-Laplace, R. Gilbin, C. Adam, C. Della-Vedova, Environ. Sci. Technol. 43 (2009) 6684.
[12] J. Bruno, R.C. Ewing, Elements 2 (2006) 343.
[13] C.J. Burns, M.P. Neu, H. Boukhalfa, K.E. Gutowski, N.J. Bridges, R.D. Rogers, in: J.A. McCleverty, T.J. Meyer (Eds.), Comprehensive Coordination Chemistry II, vol. 3, Elsevier, Amsterdam, 2003, p. 189.
[14] P.D. Beer, G.D. Brindley, O.D. Fox, A. Grieve, M.I. Ogden, F. Szemes, M.G.B. Drew, J. Chem. Soc., Dalton Trans. (2002) 3101
[15] J.D. Xu, K.N. Raymond, Inorg. Chem. 38 (1999) 308.
[16] S. Shinkai, H. Koreishi, K. Ueda, T. Arimura, O. Manabe, J. Am. Chem. Soc. 109 (1987) 6371.
[17] C.B. Ni, D.K. Shuh, K.N. Raymond, Chem. Commun. 47 (2011) 6392 (and references therein).
[18] A.C. Sather, O.B. Berryman, J. Rebek, J. Am. Chem. Soc. 132 (2010) 13572.
[19] G. Szigethy, K.N. Raymond, Inorg. Chem. 49 (2010) 6755.
[20] G. Szigethy, K.N. Raymond, Inorg. Chem. 48 (2009) 11489.
[21] R. Kannappan, D.M. Tooke, A.L. Spek, J. Reedijk, Inorg. Chim. Acta 359 (2006) 334.
[22] R. Kannappan, S. Tanase, D.M. Tooke, A.L. Spek, I. Mutikainen, U. Turpeinen, J. Reedijk, Polyhedron 23 (2004) 2285.
[23] J.L. Sessler, P.J. Melfi, G.D. Pantos, Coord. Chem. Rev. 250 (2006) 816.
[24] Y.Y. Fang, L. Wu, J.L. Liao, L. Chen, Y.Y. Yang, N. Liu, L.T. He, S.L. Zou, W. Feng, L.H. Yuan, RSC Adv. 3 (2013) 12376.
[25] K.L. Nash, Solvent Extr. Ion Exch. 11 (1993) 729.
[26] M.S. Bharara, K. Strawbridge, J.Z. Vilsek, T.H. Bray, A.E.V. Gorden, Inorg. Chem. 46 (2007) 8309.
[27] S.K. Sahu, V. Chakravortty, J. Radioanal. Nucl. Chem. 227 (1998) 163.
[28] K. Takao, Y. Ikeda, Inorg. Chem. 46 (2007) 1550.
[29] S. Chakraborty, S. Dinda, R. Bhattacharyya, A.K. Mukherjee, Z. Kristallogr. 221 (2006) 606.
[30] R. Kannappan, M.S. Bharara, K. Heflin, S. Tonks, K.L. Strawbridge, A.V.E. Gorden, Dalton Trans. (2008) 2966
[31] D.J. Evans, P.C. Junk, M.K. Smith, Polyhedron 21 (2002) 2421.
[32] A.W. Maverick, R.K. Laxman, M.A. Hawkins, D.P. Martone, F.R. Fronczek, Dalton Trans. (2005) 200
[33] S.M. Kim, J.S. Kim, D.M. Shin, Y.K. Kim, Y. Ha, Bull. Korean Chem. Soc. 22 (2001) 743.
[34] N. Fridman, M. Kaftory, Pol. J. Chem. 81 (2007) 825.
[35] V.Z. Mota, G.S.G. de Carvalho, P.P. Corbi, F.R.G. Bergamini, A.L.B. Formiga, R. Diniz, M.C.R. Freitas, A.D. da Silva, A. Cuin, Spectrochim. Acta, Part A 99 (2012) 110.
[36] X.H. Lu, Q.H. Xia, H.J. Zhan, H.A. Yuan, C.P. Ye, K.A. Su, G. Xu, J. Mol. Catal. A Chem. 250 (2006) 62.
[37] A.R. Silva, C. Freire, B. de Castro, New J. Chem. 28 (2004) 253.
[38] B.V. Nonium, Delft, The Netherlands (1998).
[39] A.J.M. Duisenberg, J. Appl. Crystallogr. 25 (1992) 92.
[40] A.J.M. Duisenberg, L.M.J. Kroon-Batenburg, A.M.M. Schreurs, J. Appl. Crystallogr. 36 (2003) 220.
[41] SAINT, Bruker-AXS, Karlsruhe, Germany (2008).
[42] APEX2, Bruker-AXS, Karlsruhe, Germany (2008).
[43] G.M. Sheldrick, Acta Crystallogr., Sect. A 46 (1990) 467.
[44] G.M. Sheldrick, SADABS: Empirical Absorption and Correction Software, University of Göttingen, Germany, 1999–2003.
[45] G.M. Sheldrick, SHELXL-97: Programs for Crystal Structure Analysis, University of Göttingen, Germany, 1997.
[46] V. Barone, M. Cossi, J. Phys. Chem. A 102 (1998) 1995.
[47] A. Bondi, J. Phys. Chem. 68 (1964) 441.
[48] M.J. Frisch, G.W. Trucks, H.B. Schlegel, G.E. Scuseria, M.A. Robb, J.R. Cheeseman, J.A. Montgomery, T. Vreven, K.N. Kudin, J.C. Burant, J.M. Millam, S.S. Iyengar, J. Tomasi, V. Barone, B. Mennucci, M. Cossi, G. Scalmani, N. Rega, G.A. Petersson, H. Nakatsuji, M. Hada, M. Ehara, K. Toyota, R. Fukuda, J. Hasegawa, M. Ishida, T. Nakajima, Y. Honda, O. Kitao, H. Nakai, M. Klene, X. Li, J.E. Knox, H.P. Hratchian, J.B. Cross, V. Bakken, C. Adamo, J. Jaramillo, R. Gomperts, R.E. Stratmann, O. Yazyev, A.J. Austin, R. Cammi, C. Pomelli, J.W. Ochterski, P.Y. Ayala, K. Morokuma, G.A. Voth, P. Salvador, J.J. Dannenberg, V.G. Zakrzewski, S. Dapprich, A.D. Daniels, M.C. Strain, O. Farkas, D.K. Malick, A.D. Rabuck, K. Raghavachari, J.B. Foresman, J.V. Ortiz, Q. Cui, A.G. Baboul, S. Clifford, J. Cioslowski, B.B. Stefanov, G. Liu, A. Liashenko, Piskorz, P.I. Komaromi., R.L. Martin, D.J. Fox, T. Keith, M.A. Al-Laham, C.Y. Peng, A. Nanayakkara, M. Challacombe, P.M.W. Gill, B. Johnson, W. Chen, M.W. Wong, C. Gonzalez, J.A. Pople, Gaussian 03, Revision D.01, Gaussian, Inc., Wallingford, CT, 2004.
[49] W. Küchle, M. Dolg, H. Stoll, H. Preuss, J. Chem. Phys. 100 (1994) 7535.
[50] R. Krishnan, J.S. Binkley, R. Seeger, J.A. Pople, J. Chem. Phys. 72 (1980) 650.
[51] H. Stephan, M. Kubeil, K. Gloe, K. Gloe, Extraction methods, in: C. Schalley (Ed.), Analytical Methods in Supramolecular Chemistry, Wiley-VCH, Weinheim, 2012, pp. 105–127.
[52] P.A. Vigato, S. Tamburini, Coord. Chem. Rev. 248 (2004) 1717.
[53] H. Holm, G.W.E. Everett Jr., A. Chakravorty, Prog. Inorg. Chem. 7 (1966) 83.
[54] A.A.A. Abu-Hussen, J. Coord. Chem. 59 (2006) 157.
[55] T.S. Franczyk, K.R. Czerwinski, K.N. Raymond, J. Am. Chem. Soc. 114 (1992) 8138.
[56] U. Casellato, S. Tamburini, P. Tomasin, P.A. Vigato, Inorg. Chim. Acta 341 (2002) 118.
[57] P.A. Giesting, P.C. Burns, Crystallogr. Rev. 12 (2006) 205.
[58] P.V. Rao, C.P. Rao, A. Sreedhara, E.K. Wegelius, K. Rissanen, E. Kolehmainen, J. Chem. Soc., Dalton Trans. (2000) 1213
[59] H.H. Freedman, J. Am. Chem. Soc. 83 (1961) 2900.
[60] G. van Koten, J. Organomet. Chem. 730 (2013) 156.